Received: 29 November 2022 | Revised: 13 April 2023 | Accepted: 10 May 2023

DOI: 10.1002/cnm.3737

WILEY

SPECIAL ISSUE ARTICLE

Patient-specific hemodynamic feature of central venous disease intervened by stent: A numerical study

Zhaoli Wang[1] | **Tao Li**[2] | **Jingyuan Zhou**[1] | **Yang Yu**[3,4] | **Yu Chen**[1] | **Ping Fu**[3,4]

[1]Department of Applied Mechanics, Sichuan University, Chengdu, China

[2]College of Mechanical Engineering, Sichuan University, Chengdu, China

[3]Kidney Research Laboratory, Division of Nephrology, West China Hospital of Sichuan University, Chengdu, China

[4]National Clinical Research Center for Geriatrics, West China Hospital of Sichuan University, Chengdu, China

Correspondence

Yang Yu, Kidney Research Laboratory, Division of Nephrology, West China Hospital of Sichuan University, Chengdu 610065, Sichuan, China.
Email: yuyang@wchscu.cn

Yu Chen, Department of Applied Mechanics, Sichuan University, Chengdu 610065, Sichuan, China.
Email: yu_chen@scu.edu.cn

Funding information

Major Research Programs of Science & Technology Department of Sichuan Province, Grant/Award Number: 2021YFS0163

Abstract

Central venous disease (CVD) with stenosis or occlusion is a severe and prevalent complication for chronic hemodialysis (HD) patients, resulting in dialysis access dysfunction. Percutaneous transluminal angioplasty with stent placement (PTS) has become one of the first-line treatments for CVD. In clinical practice, the extra stents would be used if the curative efficacy of a single stent were unsatisfactory. Aiming to evaluate the therapeutic effect of different PTS schemes, computational fluid dynamics (CFD) simulations on four patients were performed to compare the hemodynamic characteristics of real-life HD patients after stent placement. The three-dimensional central vein's models of each patient were built using computational tomography angiography (CTA) images, and idealized models were constructed as contrast. Two inlet velocity modes were imposed to imitate the blood flow rate of healthy and HD patients. The hemodynamic parameters for different patients were investigated, including wall shear stress (WSS), velocity, and helicity. The results showed that the implantation of double stents is able to improve flexibility. When subjected to external force, the double stents have better radial stiffness. This paper evaluated the therapeutic efficacy of stent placement and provided a theoretical basis for CVD intervention in hemodialysis patients.

KEYWORDS

central venous disease, endovascular intervene, hemodynamic, numerical simulation, stent

1 | INTRODUCTION

Vascular access is crucial for hemodialysis in patients with end-stage renal disease (ESRD) as it allows for adequate blood flow rates. Central venous stenotic and occlusive disease (CVD) is a serious complication for chronic hemodialysis patients, leading to vessel access obstruction, decreased blood flow, and venous hypertension. CVD has a high incidence among ESRD patients, reaching 24%–40%, and is the leading cause of dialysis access dysfunction that endangers patients' lives.[1,2]

CVD refers to the reduction of >50% of the luminal area in the superior vena cava (SVC), internal and external jugular vein (IJV/EJV), subclavian vein (SCV), and brachiocephalic vein (BCV).[3] The risk factors for CVD include chronic trauma from repeated catheter insertion and abnormally high flow volume from arteriovenous access.[4] Stenosis of

central vein may contributes to elevated peripheral venous pressure and residual symptoms, mainly ipsilateral extremity and facial edema.

Approximately 50% of patients require therapeutic interventions due to symptomatic CVD.[5] Percutaneous transluminal angioplasty (PTA) with or without stent has been the preferred approach to CVD.[6] The drawbacks of PTA only with balloons include insufficient dilation or extrusion and recoil of veins.[7] To cover these deficiencies, the stent is placed to sustain the vessel lumen and maintain the dilated state. Percutaneous transluminal angioplasty with stent (PTS) can reduce elastic recoil and lesion recurrence, prolonging the time of patency.[8]

After stent implantation, the ideal status after stent implantation can be characterized by four main factors: (1) absence of kinks along the whole stent. This avoids mechanical failure, stent fracture or dislocation, and decreases risk of restenosis; (2) smooth and continuous shape of the vessel, which is necessary for maintaining proper blood flow and minimizing the risk of thrombosis and embolism. (3) stable and undisturbed blood flow. It is crucial for maintaining proper tissue perfusion and reducing the risk of thrombosis, plaque formation, or tissue damage; and (4) absence of abnormally high or low WSS regions. It can prevent the development of intimal hyperplasia or atherosclerosis, which are major causes of restenosis and stent failure.

Despite extensive research on arterial diseases and arterial stenting, there is a lack of numerical simulations in central venous diseases and treatments. Existing studies on therapeutic efficacy are mainly based on clinical statistics, such as Dolmatch et al.[8] who conducted a clinical study of 64 patients with graft endovascular failure implanted with COVERA™, showing a good initial patency rate of 73.6% after 6 months of intervention. Some studies on computational fluid dynamics (CFD) examine the causes of vessel access stenosis. Lonyai et al.[9] constructed models with anatomic data derived from computed tomography angiography (CTA) images to perform patient-specific simulations examining blood flow velocity, WSS, and blood pressure, both with and without the presence of heart pacemaker leads. Morbiducci et al.[10] confirmed the strength of helical flow as an index for risk stratification. The existing studies on hemodynamic changes after stent placement with improved central venous lumen are limited. Chen et al.[11] constructed patient-specific geometric models with CTA images and compared pressure, wall shear stress, and flow velocity in the BCV before and after stent placement based on CFD simulation.

The ultimate goal of this study is to provide more insights into the therapeutic effect of central venous stent placement, particularly from a hemodynamic perspective. This paper performs numerical simulations using geometrical data obtained from clinical images for specific patients to ensure more realistic results. By using computational fluid dynamics simulations, we aim to explore the changes in blood flow patterns, velocity, WSS, and helicity in the central veins before and after stent implantation. This will help us understand the factors that contribute to stent efficacy and to optimize the design of future venous stents.

2 | METHODS

2.1 | Patient

The patient-specific database of hemodialysis patients with central vein stenosis or occlusion from June 2017 to April 2021 was reviewed in this study, provided by the West China Hospital of Sichuan University (Chengdu, Sichuan, China). Four typical patients treated with PTS were selected to consist the study group. The basic information and endovascular treatment procedure of them are shown in Table 1. The CTA images are shown in Figure 1. One patient (patient 1) was implanted with a single stent, the other three patients with two stents. Patient 2 have had intervention with two partly overlapped stents at the very beginning. Patient 3 and Patient 4 received only one stent at first, and required placement of another nested stent to achieve recanalization.

TABLE 1 The basic and stent-implanting information of patient.

Patients	Age	Sex	Focal position	Procedure
1	55	M	RBCV	Single stent
2	67	F	RBCV	Two overlapped stents
3	56	M	LSCV	Two nested stents
4	78	F	LBCV	Two nested stents

If the stenosis or occlusion occurs, where the BCV drains from SCV and IJV, the stent would be placed to recanalize the access from SCV to BCV，and IJV would be blocked. There would be no more blood flow from IJV to BVC. Patient 1, 2, 3 all have the absence of unilateral IJV (Figure 1).

2.2 | Model

Patient-specific data sets included thoracic computed tomography angiography (CTA) images and 2-dimensional digital substruction angiography (2D-DSA) images and videos. The CTA images was scanned by CT X-ray (SOMATOM Definition Flash, SIEMENS, slice thickness is 1.0 mm). Patient-specific three-dimensional geometry were obtained from CTA images using commercially available software Mimics (version 21.0; Materialize, Plymouth, Mich).

External jugular vein, azygous vein, and so forth. were excluded to simplify the simulation process. Stents were regarded as being completely coherent with vessel wall. The lumen of stent equal to vessel lumen.

All the models used in this study are shown in Figure 2, including four Patients and nine models. The single or double model were digitized directly from CTA images. To set up an idealized model as contrast, optimized models were constructed. The specific method to construct optimized model is: 1. Reconstruct the central vein of patient with lesion

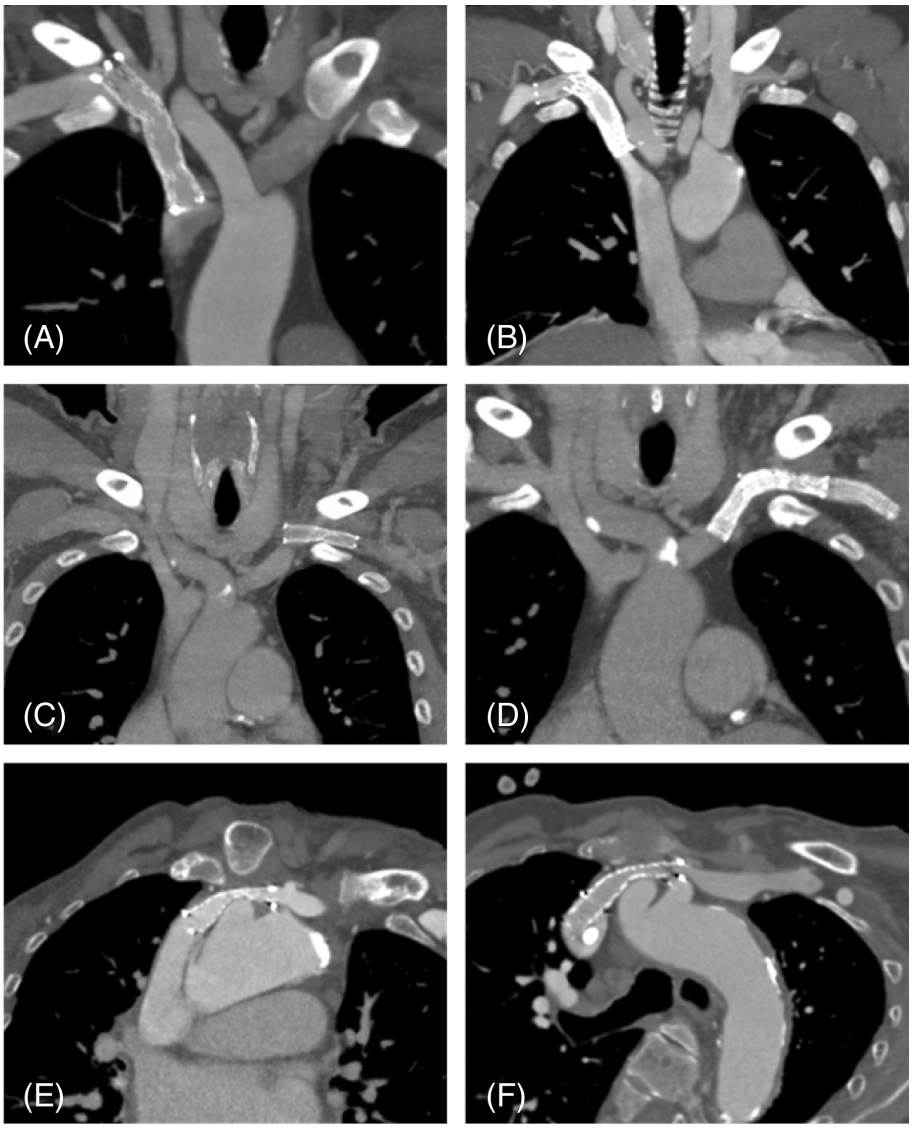

FIGURE 1 The CTA images of four patients. (A) Patient 1 with a single stent. (B) Patient 2 with two overlapped stents. (C) Patient 3 with the first stents. (D) Patient 3 with two nested stents. (E) Patient 4 with the first stent. (F) Patient 4 with two nested stents.

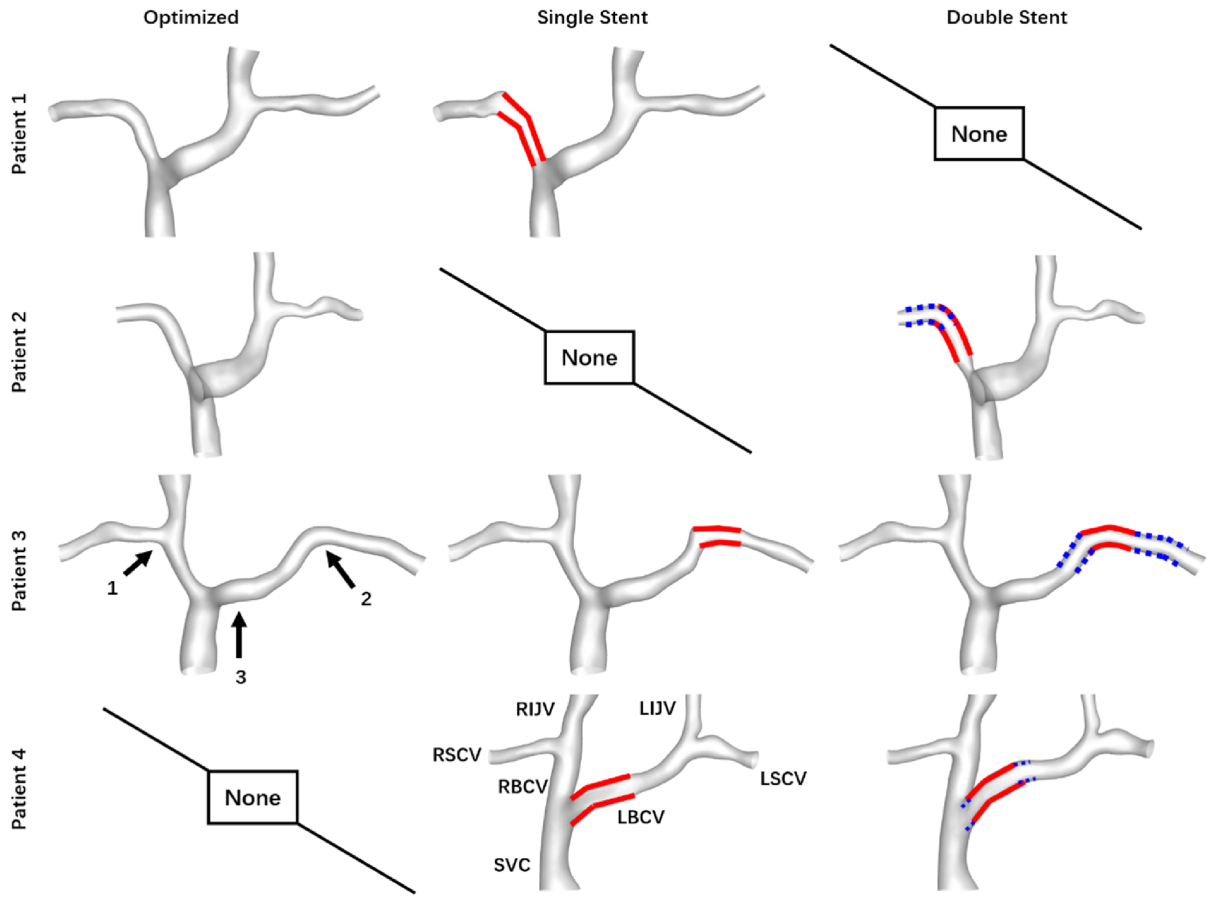

FIGURE 2 All the model of four patients. The red solid line shows the position of single stent or the first stent, the blue dash line represents the position of second stent; The end of stent near superior vena cava called proximal end, the other is distal end; RSCV/LSCV, Right/Left subclavian vein; RIJV/LIJV , Right/Left internal jugular vein; RBVC/LBCV , Right/Left brachiocephalic vein; SVC , Superior vena cava; Arrow 1 and Arrow 2 note the curvatures on coronal plane; Arrow 3 notes the curvature on transverse plane.

before PTS, and extract the centerline of the lesion part; 2. Draw a circle with a radius equal to the nearby vessel of the lesion and sweep it along centerline to create a new vessel segment; 3. Cut off the stent segment of stent model and replace it with the newly created vessel segment; 4. Connect them properly, adjust and smooth the joint. The optimized model was established. It was assumed that optimized model represented an idealized stenting situation, where the flexibility and radial stiffness were both excellent, and the vein is smooth. Optimized model would be the control group in follow-up simulation and analysis.

The anatomic geometry of central vein is asymmetric. Shown as Figure 2, in the right lateral, RSCV meets RIJV and forms RBCV, and down to the SVC straightly. There is only one curvature in the coronal plane (Arrow 1). In the left lateral, LBCV needs to bypass the brachiocephalic trunk to flow into SVC. Consequently, after the curvature in the coronal plane (Arrow 2), there is another curvature in transverse plane (Arrow 3). Hence, the blood flow is different in two side.

The lesions and stents locate at the vessel's curvature in patient 1, 2 and 3, the key point of which is the flexibility. These cases mainly discuss the distribution of WSS, flow streamline, velocity and helicity. However, the pathogenesis is much different for patient 4's stenosis. It is caused by the compression of sternum and brachiocephalic artery so the emphasis is the radial stiffness of stent. The single-stent and double-stent model are both smooth and the most significant distinction between them is the vessel lumen area. Hence, we focus on the flow streamline and pressure drop of whole central vein in patient 4.

2.3 | Numerical simulation

In this study, blood was assumed to be set as an incompressible, homogeneous and Newtonian fluid. There are previous studies revealed that the distribution of pressure and velocity showed much higher values with respect to time and

location in large and middle vessels.[12] Furthermore, this study aims to make comparison among optimized, single-stent and double-stent model. The difference between Newtonian and non-Newtonian could be omitted.

The governing equations are written as follows:

$$\nabla \cdot \vec{u} = 0 \tag{1}$$

$$\rho\left(\frac{\partial \vec{u}}{\partial t} + \vec{u} \cdot \nabla \vec{u}\right) = -\nabla p + \mu \nabla^2 \vec{u} \tag{2}$$

Where $\vec{u}$ is the blood velocity, p the static pressure. ρ and μ are the density and dynamic viscosity, were set to be 1050 kg/m^3 and 3.5×10^{-3} kg/m·s respectively in the simulation.

The three-dimensional models were spatially discretized into unstructured polyhedral elements, and locally refined in stent-implanted area, shown in Table2 specifically. Then they were solved by finite volume method using CFD software (ANSYS FLUENT 2022 R1, ANSYS, Inc., Canonsburg, PA, USA). The solver was set to be laminar and steady.

After calculation, the visualization and analysis of blood flow field were completed by post-processing software (Tecplot 2018 R1, Tecplot, Inc., Bellevue, WA, USA). The variables analyzed in post-process included WSS, flow streamline, velocity magnitude, pressure and local normalized helicity (LNH). LNH is a dimensionless number that physically represents the angle between velocity and vorticity vectors, indicating the strength of helical flow:

$$LNH = \frac{\vec{u} \cdot \vec{\omega}}{\left|\vec{u}\right|\left|\vec{\omega}\right|} \quad -1 \le LNH \le 1 \tag{3}$$

Theoretically, the smaller absolute value of LNH is, the more tendencies to purely axial flow, otherwise the swirling flow. It can be inferred that large and continuous region with high LNH indicates the helical flow. If the high LNH region is scattered, fragmentized, and even flipping between positive and negative, the flow would be irregular and disordered.[13]

2.4 | Boundary condition

Patient-specific data was not used as boundary condition. Instead, there are two modes of boundary conditions. One is low flow rate, which represents the normal blood flow, the other is high flow rate set to simulate the flow of hemodialysis.

In the low flow rate mode, the velocity at the SCV is set to be .08 m/s, and the flow rate is calculated based on the vessel section area at the inlet. It's assumed that the flow split between the SCV and IJV was equal,[9] so the inlet velocity at the IJV is calculated based on the flow rate of SCV and the area of IJV. In the high flow rate mode, the inlet velocities

TABLE 2 Element number of models.

Patient	Model	Total elements number	Elements number of stent
1	Optimized model	280,627	186,941
	Single model	607,928	406,818
2	Optimized model	285,673	72,504
	Double model	284,509	72,598
3	Optimized model	371,367	159,673
	Single model	363,563	150,259
	Double model	187,224	81,647
4	Single double	327,995	88,409
	Double model	260,229	99,326

remain unchanged, except for the SVC that drains blood from AVF which is set to be .24 m/s to simulate the high flow rate of hemodialysis.

Under this inlet velocity setting scheme, the sum of bilateral SCV flow rate of 4 patients ranged from 737.6 to 1183.4 mL/min, and the total flow rate in SVC varied between 1475.3 and 2366.78 mL/min. The flow rate in vessel access with AVF ranged from 1365.455 to 1813.57 mL/min. The flow rate were all in reasonable and physiological range.[14–17]

The 0-pressure outlet boundary condition was imposed in the exit of SVC, and the lumen walls were assumed to be rigid and non-slip.

3 | RESULTS

The stent of Patient 1 covered the curvature from RSCV to RBCV. Due to the bad compliance, it was hard to curve. The stent kinked and deformed the vein. The focal stenosis of Patient 2 was the same as Patient 1, but with an extra stent in first stent's distal end to bend it and fit the geometry of vein. The lesion of Patient 3 was situated in the cross of LSCV and LIJV. It was recanalized through LSCV to LBSV, and the LIJV was occluded. The lesion of Patient 4 was in the curvature of LBCV around brachiocephalic trunk. Single stent was implanted at first, it did not fully open because of compression between the sternum and enlarged brachiocephalic trunk. The lumen area was 92.97mm^2. The second stent was implanted inside the first one after 9 months and the lumen area dilated to 137.67 mm^2.

3.1 | Wall shear stress

WSS is an important hemodynamic parameter related to the pathology of vessel stenosis. The WSS higher than 3 Pa and lower than .1 Pa is considered to be abnormal.[18,19] The implantation of stent forms the curvature of vein and luminal cross-section shape, which may be unsmooth and irregular if the flexibility of stent is incompatible with vessel compliance. We analyzed four patient cases and found that the maximum and minimum WSS occurred at different locations, depending on the patient and the type of stent used. As shown in Figure 3, the distribution of WSS is conspicuously relevant to the vessels' geometry. To quantitatively analyze the WSS in detail, Figure 4 depict the distribution of WSS of Patient 1, 2, 3 along the paths noted in Figure 5.

Patient 1: The indentation observed in Figure 3A (Arrow 4) is a result of the compression of the clavicle. The maximum is located in the indentation and the minimum lied in the distal end of stent. In high flow rate mode, the single-stent model showed higher overall WSS compared to the optimized model, with a maximum WSS of 4.96 Pa observed, 2.86 Pa higher than that of the optimized model. The WSS in the low region of the single-stent model was lower at .063 Pa, .38 Pa lower than optimized model;

Patient 2: Venous geometry is much smoother due to the presence of two overlapped stents, and the distinctions of WSS between two models are minor;

Patient 3: Compared to optimized model, the single-stent model exhibits prominent high WSS regions (Figure 3C, Arrow 5) and low WSS regions (Figure 3C, Arrow 6), while the double-stent model shows a milder WSS distribution. In high flow rate mode, the maximum is 4.5 Pa (Figure 3C, Arrow 5) in the single-stent model which is 1.0 and .8 Pa higher than that of the optimized model and double-stent model respectively, and the values of low region range from .02 to .1 Pa. The WSS distribution in double-stent model and optimized model is similar, with values generally higher than .1 Pa basically;

Patient 4: The maximum of single stent model is 4.78 Pa (Figure 3D, Arrow 7), higher than the that of double stent model (3.00 Pa, Figure 3D, Arrow 8). And the area of region with WSS lower than .1 Pa is larger than double-stent model.

Generally, the high flow rate increases the magnitude of WSS in average across all models, particularly in narrow or pointy regions. However, the value in low WSS region do not evaluate much. However, the low WSS regions do not seem to be affected as much. The presence of vessel geometry discontinuities increases the likelihood of abnormal WSS regions forming. In the high flow rate mode, the single-stent models exhibited larger abnormal WSS regions compared to the double-stent and optimized models. Specifically, the maximum WSS in the single-stent models exceeded 3 Pa, whereas the WSS in the double-stent and optimized models remained below 3 Pa.

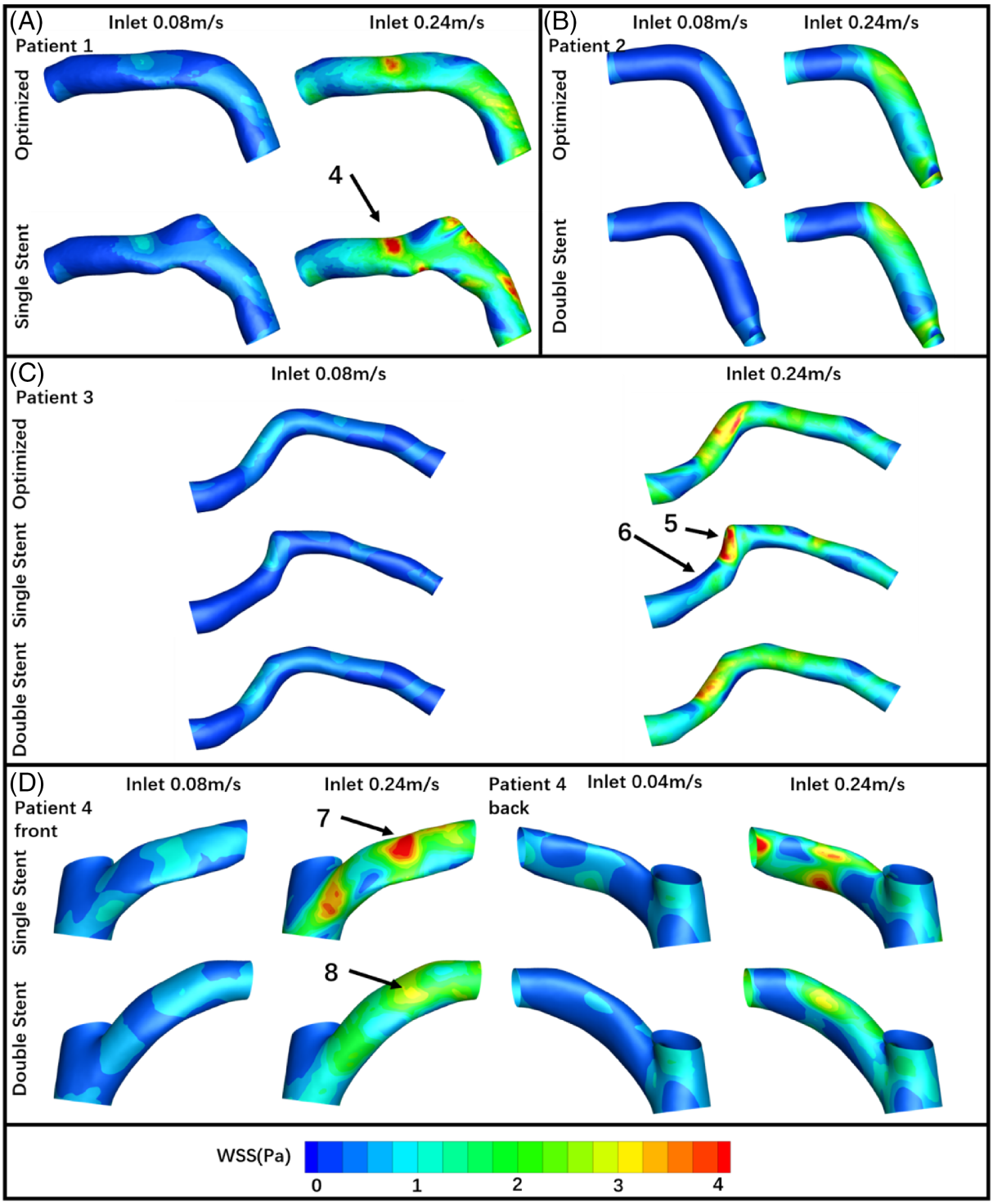

FIGURE 3 WSS counter under different inlet velocity and models. Arrow 4 points the indentation compressed by clavicle; Arrow 5 notes the high WSS region and Arrow 6 notes the low WSS region of patient 3's single-stent model; Arrow 7 and Arrow 8 point the maximum WSS in single-stent model and double-stent model representatively.

3.2 | Flow pattern

The velocity magnitude, flow streamline and distribution of LNH are utilized to describe the flow pattern. Figure 6 illustrates the flow streamline in two different flow rate modes, where the color of the streamline represents the velocity

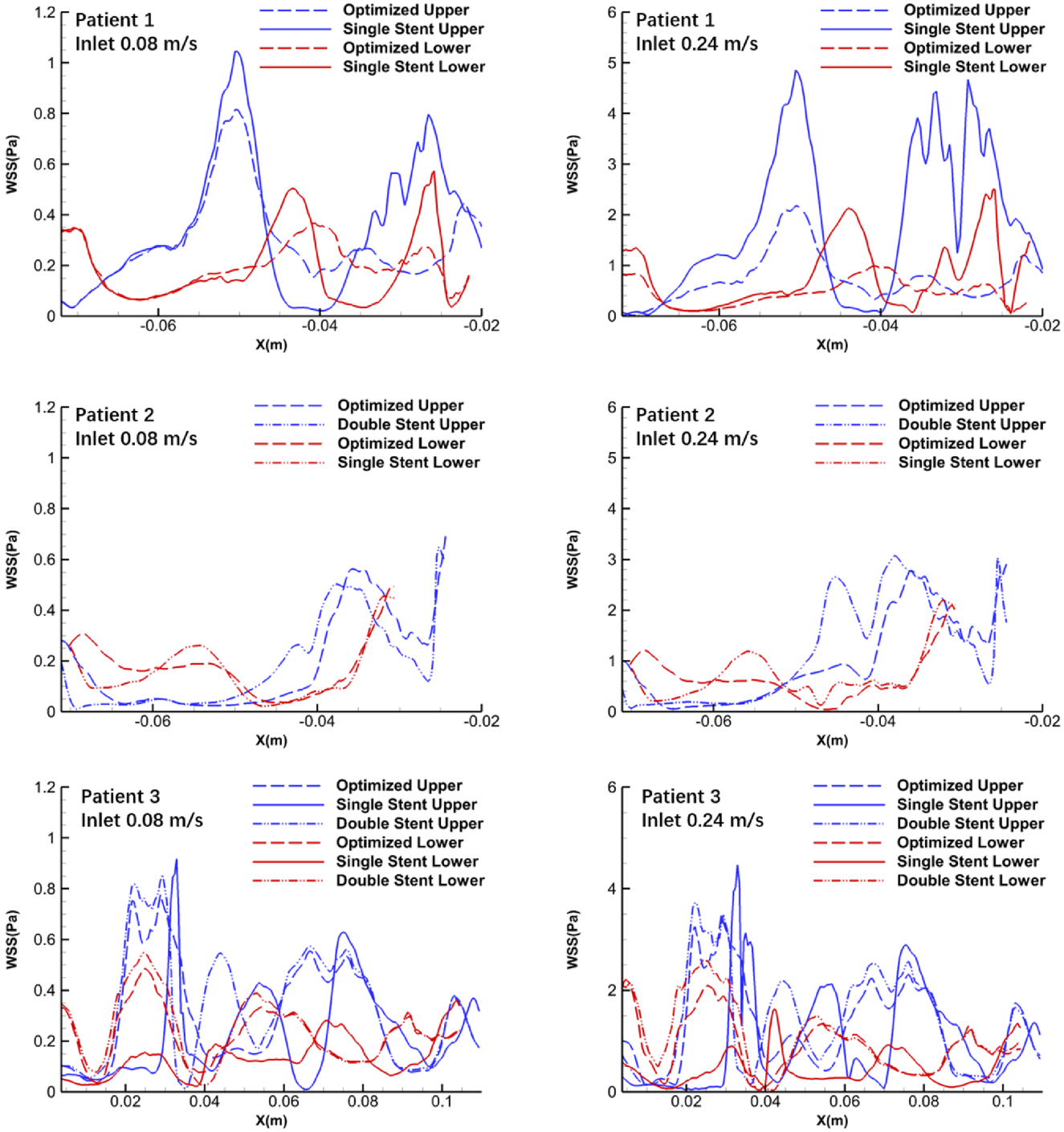

FIGURE 4 WSS distribution along the paths noted in Figure 5. Blue line represents the upper path; red line represents the lower path.

magnitude. The distribution of the velocity magnitude in a typical section is shown in Figure 7 for an inlet velocity of .24 m/s. Figure 8 depicts the contour map of LNH for Patient 1, 2, and 3.

For single-stent model in Patient 1, the velocity magnitude is higher than optimized model in the distal end and curvature, the streamline is disordered. The high LNH region become fragile and reversed region increases; However, the double-stent in Patient 2 have little influence in flow pattern; For Patient 3, the velocity magnitude of the single-stent model was higher than the optimized model in the distal end, but it decreased significantly in the stenting segment of LBCV. The LNH flipped between positive and negative, indicating the intertwining of counter-rotating flow. After the second stent is implanted, the negative LNH diminish and the flow pattern inside the lumen become similar with optimized model.

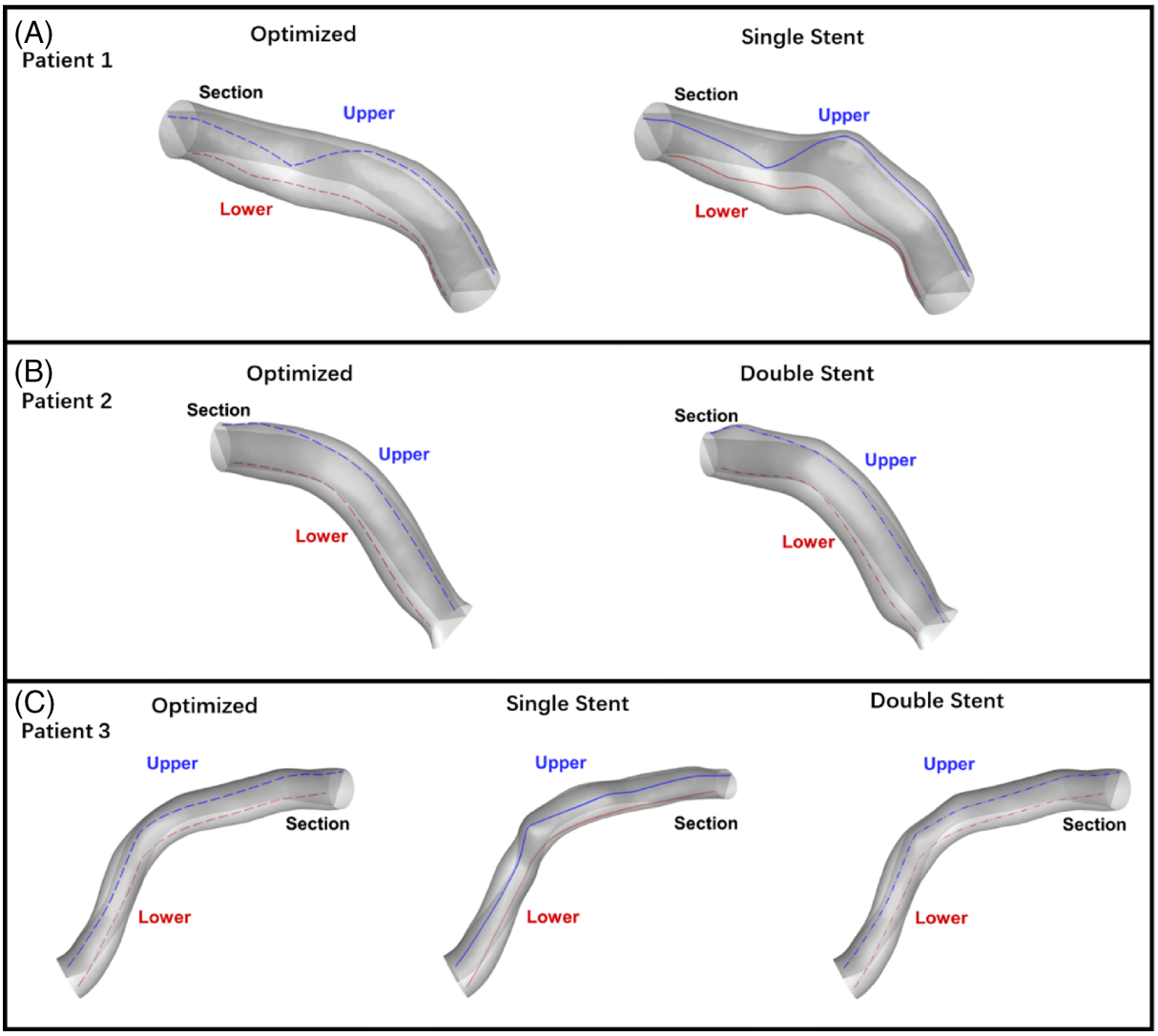

FIGURE 5 The position of typical sections and WSS distribution paths (Upper/Lower).

In Patient 4, the second stent dilated the luminal area, which mainly changes the flow upstream. Figure 6D shows the flow streamline and velocity magnitude of the entire central vein. When the flow rate is low, the flow patterns between two models have no significant difference, except in the sinus in LSCV (Arrow 9), where the recirculation of single-stent model is more prominent. When the flow rate is high, due to the narrowness in LBCV in single-stent model, the velocity is faster and the flow of LBCV wash out the wall of SVC (Arrow 10). In contrast, the flow gathered into flow of SVC in double-stent model.

To summarize, the flow pattern in double-stent model is similar to optimized model. The geometries of single-stent models are more likely to generate the adverse flow pattern such as distorted streamline and discontinuous or intertwined high LNH region.

3.3 | Differential pressure

A serious symptoms of venous hypertension caused by CVD is edema of ipsilateral extremity and face. To evaluate the improvement brought by stent placement, the Figure 9 gives the differential pressure (DP) between LSCV/LIJV and SVC in different model and inlet velocity. LSCV drains the blood from left upper limb and LIJV drains the cerebral blood. In high flow rate mode, the DP of LSCV in the single-sent model is 217 Pa, almost 3 times that of double-stent model, but the distinction of DP of LIJV is tiny. In low flow stent mode, DP in both veins of the single-stent model is only slightly higher than double-stent model.

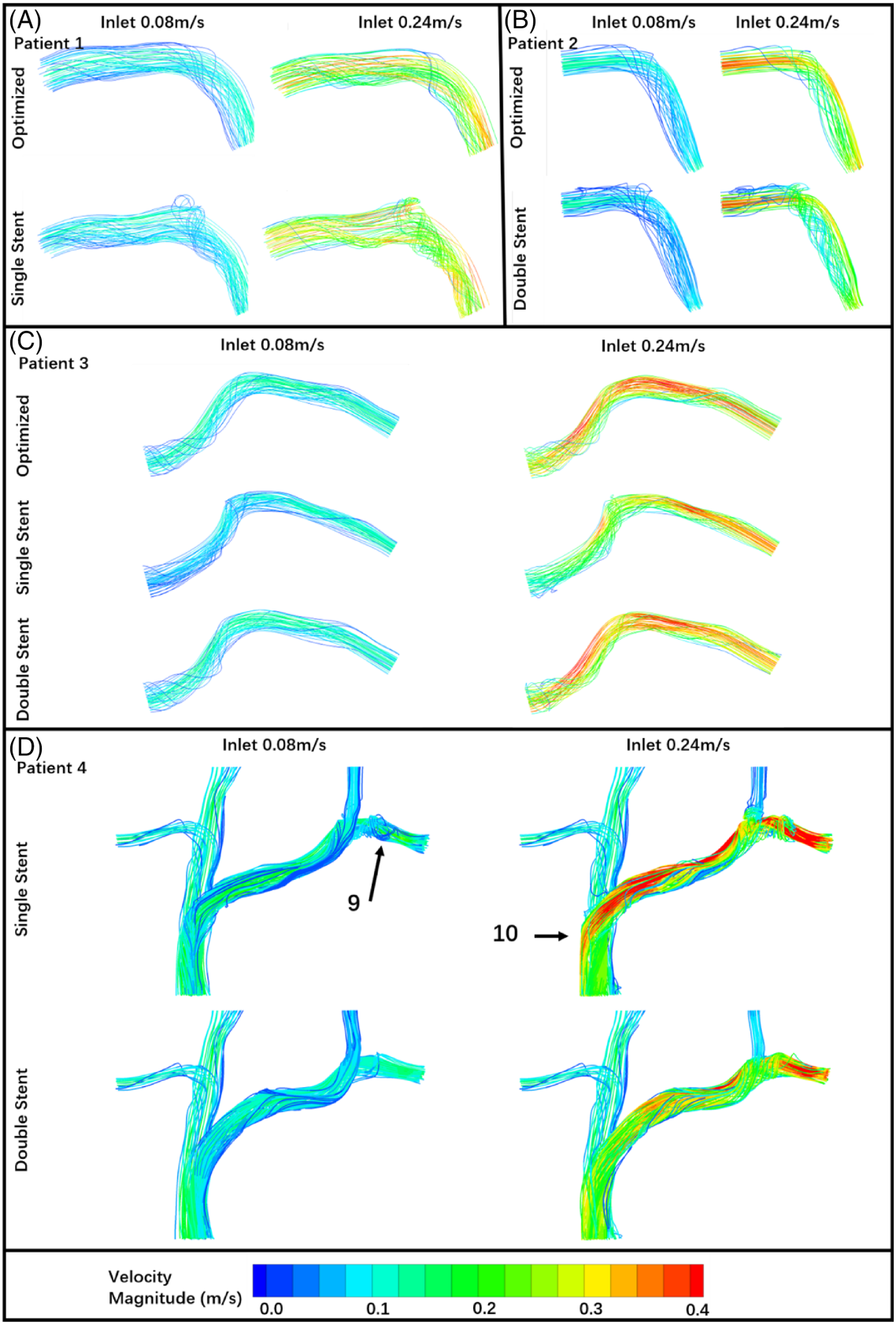

FIGURE 6 Flow streamlines and velocity magnitude. Arrow 9 notes the blood recirculation in the sinus; Arrow 10 points that the flow of LBCV wash out the wall of SVC.

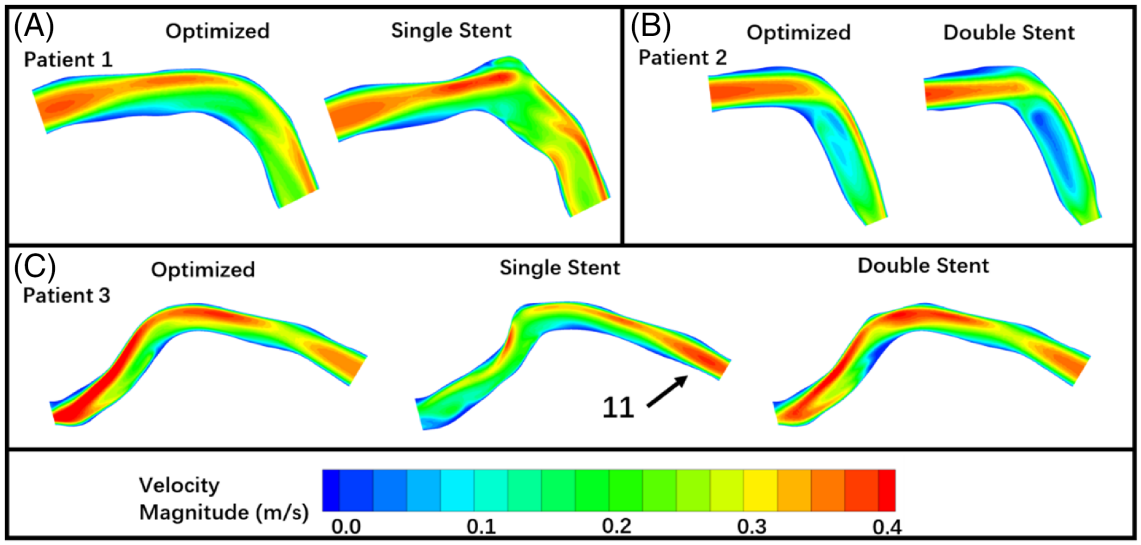

FIGURE 7 Velocity magnitude contour maps when the inlet velocity is .24 m/s. It shows the distribution in typical section noted in Figure 5. Arrow 9 points to the high velocity magnitude in the distal end of single stent.

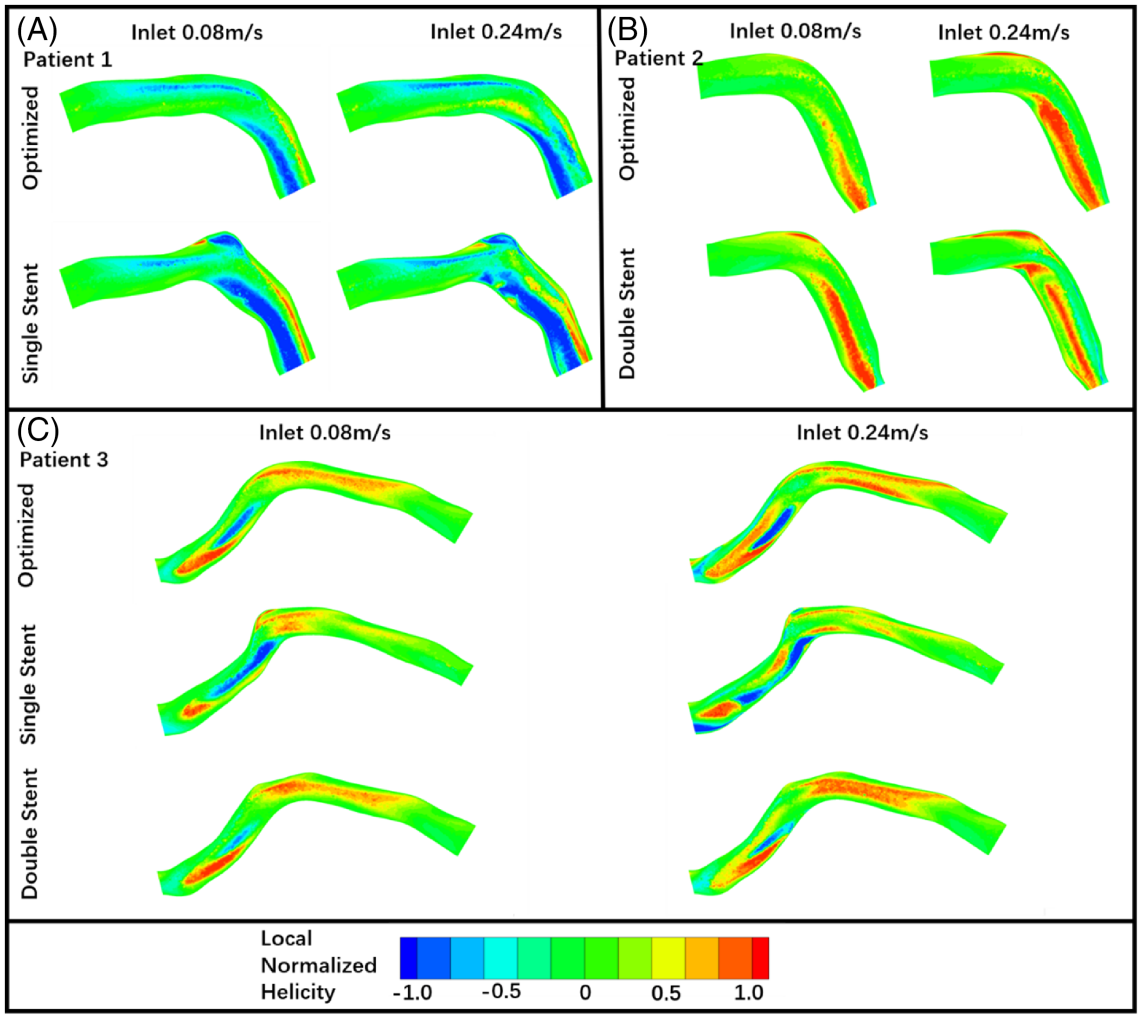

FIGURE 8 LNH contour maps. It shows the distribution in typical section noted in Figure 5.

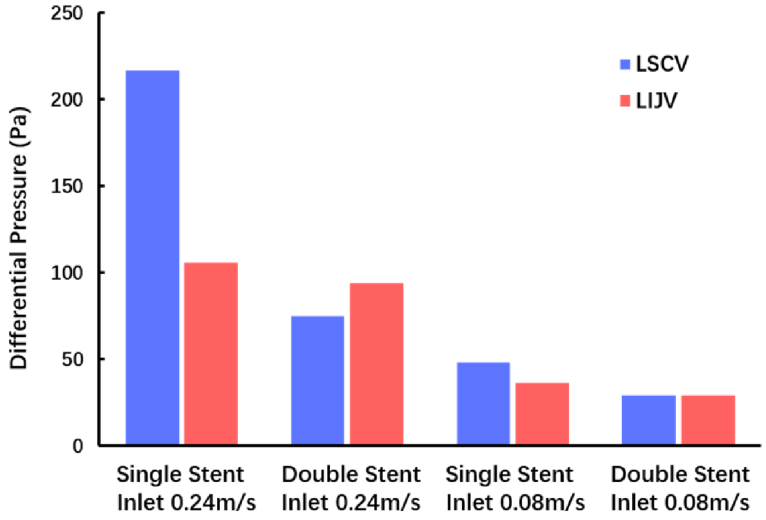

FIGURE 9 Differential pressure between LSCV or LIJV and SVC of Patient 4.

4 | DISCUSSION

The patient-specific three-dimensional geometries were acquired from CTA images, including idealized model and different stent model. Hemodynamic simulations were conducted under different inlet velocities, based on the physiological blood flow rate range of healthy individuals and HD patients. The transformations of vessels after stent placement were depicted, and the flow features and patterns were simulated and analyzed.

The results indicate that the flexibility, radial rigidity, and implanting method have impact on the hemodynamic. Low-flexibility stents may kink when placed in the curvature of central veins, leading to sharp and discontinuous vessel lumens, especially in stent ends. For single-stent models in this study, the maximum WSS is higher and minimum is lower and the area of abnormally high and low WSS regions is larger. Additionally, the inordinance geometry spoil the regular and one-directional helicity flow, leading to helicity reverse, recirculation, and stasis, especially in high flow rate status. To improve the performance of a single stent, another stent was implanted either partly overlapped or completely nested. The results demonstrate that the features of double-stent models and optimized models are similar. This operation can improve performance and address the poor compliance of a single stent. In addition, adequate radial stiffness is also pivotal for venous stents. Unlike arteries, the vein wall is thin and non-elastic, making it easily compressed by the surrounding anatomy, such as osteal structures, ligaments, and pulsating arteries. The results of Patient 4 show that a single stent is incapable of resisting the compression between the sternum and brachiocephalic artery. The second nested stent reinforced the support to the vessel wall, dilated the vessel lumen, and reduced the pressure of SCV markedly by slowing down the flow velocity. This leads to remission from edema symptoms, particularly in the upper limb. However, from the perspective of stent design, flexibility and radial rigidity may be mutually exclusive. It is essential to balance both for the research and development of venous stents.

The main reason for PTS failure is in-stent restenosis (ISR). The most common genesis of ISR in hemodialysis vascular access is exuberant neointimal hyperplasia (NIH), leading to decreasing vessel luminal patency.[20,21] The repair of vessel endothelium might be excessive, resulting in the migration of smooth muscle cells (VSMCs) from the media to the intima, eventually forming NIH.[22] The clinical researches show that most people with CVD secondary to peripherally inserted catheters, central venous port catheters, pacemaker and defibrillator leads, are usually asymptomatic but present clinically after a hemodynamic change, such as placement of an ipsilateral AV access.[23–27] Hence, it is hypothetical that the process of development of excessive NIH is divided into two steps: (1) The enthetic object causes serious endothelial injury, like central catheters, pacemaker leads, defibrillator wires and so on; (2) When the endothelium is self-rehabilitating, the abnormal hemodynamic situation induces the immoderate proliferation. Focus on ISR of central venous endovascular intervention with stent, the interventional trauma is inevitable in the process of stent implanting. The adverse hemodynamic promote the NIH, leading to ISR.

Abnormally high shear stress can result in an increase in the production of free radicals and its downstream products is inducer of the matrix metalloproteinases (MMPs)[28] which facilitate the migration of VSMCs.[29] Co-localization of

oxidative stress markers with inflammatory cytokines such as transforming growth factor-beta (TGF-β) and platelet-derived growth factor (PDGF) has also been observed,[30] contributing to NIH. On the other hand，low shear stress contributes to phenotype switching of VSCMs in vessel media.[31] In general, both extremely high or low WSS are detrimental to maintaining the patency rate. As regard to LNH, it is believed that spiral of swirling flow could resist disturbance and eliminating oscillation,[32] which could allow prolonged contact of the vessel wall with hemocytes and metabolites that may contribute to ISR.[33] High LNH regions need to be coherent, meaning a continuous and regular helical flow that can stabilize the flow field. Therefore, the use of a double stent can suppress NIH by maintaining a centralized and predominating one-vortex secondary flow.

5 | LIMITATION

Some potential limitations deserve to be point out. First, the stent was simplified as a part of vessel wall. The influence of stent applied to local microflow was not taken into consideration. Second, the flow is steady. Although the pulsatile amplitude is quite low, the ISR might attributed to the hemodynamic change caused by pulsation. Third, as mentioned before, except hemodynamics challenge, the deformation and damage of vessel wall is also crucial to restenosis. However, the vessel wall was regarded as rigid, the tensile strain and impairment was ignored in this study.

6 | CONCLUSION

In this study, we constructed patient-specific models and conducted numerical simulations to evaluate the effectiveness of venous stents in treating CVD. The results suggest that the flexibility of stents can have a significant impact on hemodynamic conditions, potentially promoting ISR, while insufficient radial stiffness may not adequately resolve symptoms of venous hypertension. The results also suggest that double stents can be a viable alternative when single stents are insufficient. These findings provide valuable therapeutic insights for clinical practice and could inform the design of future venous stent technologies. Additionally, our study can serve as a basis for further research into restenosis in CVD and guide the identification of parameter ranges for such studies.

ACKNOWLEDGEMENT

This work is supported by the Major Research Programs of Science & Technology Department of Sichuan Province (Grant No. 2021YFS0163).

CONFLICT OF INTEREST STATEMENT

The authors declare no conflicts of interest.

DATA AVAILABILITY STATEMENT

The data that support the findings of this study are available on request from the corresponding author. The data are not publicly available due to privacy or ethical restrictions.

ORCID

Yu Chen https://orcid.org/0000-0002-8931-8079

REFERENCES

1. Lumsden A. Central venous stenosis in the hemodialysis patient: incidence and efficacy of endovascular treatment. *Cardiovasc Surg*. 1997;5:504-509.
2. Glanz S, Gordon DH, Lipkowitz GS, Butt KM, Hong J, Sclafani SJ. Axillary and subclavian vein stenosis: percutaneous angioplasty. *Radiology*. 1988;168:371-373.
3. Park HS, Choi J, Baik JH. Central venous disease in hemodialysis patients. *Kidney Res Clin Pract*. 2019;38:309-317.
4. Modabber M, Kundu S. Central venous disease in hemodialysis patients: an update. *Cardiovasc Intervent Radiol*. 2013;36:898-903.
5. Schwab SJ, Quarles LD, Middleton JP, Cohan RH, Saeed M, Dennis VW. Hemodialysis-associated subclavian vein stenosis. *Kidney Int*. 1988;33:1156-1159.
6. Lok CE, Huber TS, Lee T, et al. KDOQI Clinical Practice Guideline for Vascular Access: 2019 Update. *Am J Kidney Dis*. 2020;75:S1-S164.

7. Agarwal AK. Endovascular interventions for central vein stenosis. *Kidney Res Clin Pract*. 2015;34:228-232.
8. Dolmatch B, Waheed U, Balamuthusamy S, et al. Prospective, multicenter clinical study of the Covera vascular covered stent in the treatment of stenosis at the graft-vein anastomosis of dysfunctional hemodialysis access grafts. *J Vasc Interv Radiol*. 2022;33:479-488.e3.
9. Lonyai A, Dubin AM, Feinstein JA, Taylor CA, Shadden SC. New insights into pacemaker Lead-induced venous occlusion: simulation-based investigation of alterations in venous biomechanics. *Cardiovasc Eng*. 2010;10:84-90.
10. Morbiducci U, Ponzini R, Grigioni M, Redaelli A. Helical flow as fluid dynamic signature for atherogenesis risk in aortocoronary bypass. A numeric study. *J Biomech*. 2007;40:519-534.
11. Chen B, Dai H, Yang J, et al. Computational fluid dynamics simulation of hemodynamic changes in a hemodialysis patient with central venous stenosis treated with stent. *Semin Dial*. 2022;35:528-533.
12. Rani HP, Sheu TWH, Chang TM, Liang PC. Numerical investigation of non-Newtonian microcirculatory blood flow in hepatic lobule. *J Biomech*. 2006;39:551-563.
13. Browne LD, Walsh MT, Griffin P. Experimental and numerical analysis of the bulk flow parameters within an arteriovenous fistula. *Cardiovasc Eng Tech*. 2015;6:450-462.
14. Mohiaddin RH, Wann SL, Underwood R, Firmin DN, Rees S, Longmore DB. Vena caval flow: assessment with cine MR velocity mapping. *Radiology*. 1990;177:537-541.
15. Manuel Valdueza J, von Münster T, Hoffman O, Schreiber S, Max Einhäupl K. Postural dependency of the cerebral venous outflow. *The Lancet*. 2000;355:200-201.
16. Ozen O, Unal O, Avcu S. Flow volumes of internal jugular veins are significantly reduced in patients with cerebral venous sinus thrombosis. *CNR*. 2014;11:75-82.
17. Oguzkurt L, Tercan F, Yıldırım S, Torun D. Central venous stenosis in haemodialysis patients without a previous history of catheter placement. *Eur J Radiol*. 2005;55:237-242.
18. Choi YK, Shin HJ, Kim JT, Ryou HS. Investigation on the effect of hematocrit on unsteady hemodynamic characteristics in arteriovenous graft using the multiphase blood model. *J Mech Sci Technol*. 2015;29:2565-2571.
19. Van Tricht I, De Wachter D, Tordoir J, Verdonck P. Comparison of the hemodynamics in 6 mm and 4–7 mm hemodialysis grafts by means of CFD. *J Biomech*. 2006;39:226-236.
20. Patel RI, Peck SH, Cooper SG, et al. Patency of Wallstents placed across the venous anastomosis of hemodialysis grafts after percutaneous recanalization. *Radiology*. 1998;209:365-370.
21. Salman L, Asif A. Stent graft for nephrologists: concerns and consensus. *CJASN*. 2010;5:1347-1352.
22. Lee T, Roy-Chaudhury P. Advances and new Frontiers in the pathophysiology of venous neointimal hyperplasia and dialysis access stenosis. *Adv Chronic Kidney Dis*. 2009;16:329-338.
23. Gonsalves CF, Eschelman DJ, Sullivan KL, DuBois N, Bonn J. Incidence of central vein stenosis and occlusion following upper extremity PICC and port placement. *Cardiovasc Intervent Radiol*. 2003;26:123-127.
24. Trerotola SO, Kuhn-Fulton J, Johnson MS, Shah H, Ambrosius WT, Kneebone PH. Tunneled infusion catheters: increased incidence of symptomatic venous thrombosis after subclavian versus internal jugular venous access. *Radiology*. 2000;217:89-93.
25. Korzets A, Chagnac A, Ori Y, Katz M, Zevin D. Subclavian vein stenosis, permanent cardiac pacemakers and the Haemodialysed patient. *Nephron*. 1991;58:103-105.
26. Sticherling C, Chough SP, Baker RL, et al. Prevalence of central venous occlusion in patients with chronic defibrillator leads. *Am Heart J*. 2001;141:813-816.
27. Beathard GA. Percutaneous transvenous angioplasty in the treatment of vascular access stenosis. *Kidney Int*. 1992;42:1390-1397.
28. Lehoux S. Redox signalling in vascular responses to shear and stretch. *Cardiovasc Res*. 2006;71:269-279.
29. Rotmans JI, Velema E, Verhagen HJM, et al. Matrix metalloproteinase inhibition reduces intimal hyperplasia in a porcine arteriovenous-graft model. *J Vasc Surg*. 2004;39:432-439.
30. Weiss MF, Scivittaro V, Anderson JM. Oxidative stress and increased expression of growth factors in lesions of failed hemodialysis access. *Am J Kidney Dis*. 2001;37:970-980.
31. Mondy JS, Lindner V, Miyashiro JK, Berk BC, Dean RH, Geary RL. Platelet-derived growth factor ligand and receptor expression in response to altered blood flow In vivo. *Circ Res*. 1997;81:320-327.
32. Wen J, Zheng T, Jiang W, Deng X, Fan Y. A comparative study of helical-type and traditional-type artery bypass grafts: numerical simulation. *ASAIO J*. 2011;57:399-406.
33. Chen Z, Fan Y, Deng X, Xu Z. Swirling flow can suppress flow disturbances in endovascular stents: a numerical study. *ASAIO J*. 2009; 55:543-549.

How to cite this article: Wang Z, Li T, Zhou J, Yu Y, Chen Y, Fu P. Patient-specific hemodynamic feature of central venous disease intervened by stent: A numerical study. *Int J Numer Meth Biomed Engng*. 2023;e3737. doi:10.1002/cnm.3737